Ventilation of the Subtropical North Pacific: The Shallow Salinity Minimum

LYNNE D. TALLEY

University of California-San Diego, Scripps Institution of Oceanography, La Jolla, CA 92093

(Manuscript received 26 October 1984, in final form 5 February 1985)

ABSTRACT

The shallow salinity minimum of the subtropical North Pacific is shown to be a feature of the ventilated, wind-driven circulation. Subduction of low salinity surface water in the northeastern subtropical gyre beneath higher salinity water to the south causes the salinity minimum. Variation of salinity along surface isopycnals causes variations in density and salinity at the minimum.

A model of ventilated flow is used to demonstrate how the shallow salinity minimum can arise. The model is modified to account for nonzonal, realistic winds; it is also extended to examine the three-dimensional structure of the western shadow zone. The boundary between the subtropical and subpolar gyres is given by the zero of the zonal integral of Ekman pumping. The western shadow zone fills the subtropical gyre at the base of the ventilated layers and decreases in extent with decreasing density. For parameters appropriate to the North Pacific, the eastern shadow zone is of very limited extent.

Observations of salinity and potential vorticity within and below the ventilated layer bear out model predictions of the extent of the western shadow zone.

1. Introduction

Minima and maxima of properties in the ocean pique our curiosity as they stand out against an otherwise boring, monotonic background. We tend to attach special significance to extrema, rightly or wrongly, and attempt to understand why they exist. Use of extrema as tracers of ocean flow is appealing especially in regions where direct current measurements are wanting. Although extrema are important for drawing attention to features of the circulation, one must be cautious in attaching great significance to extrema in and of themselves since the extremal property may involve unknown mixing processes and time dependence as well as circulation.

The North Pacific Ocean has several well-defined vertical salinity minima south of the Subarctic Front. The salinity minima have traditionally been divided into three groups in accordance with their origins: the shallow salinity minimum, North Pacific Intermediate Water at a density of approximately 26.8 mg ml^{-1} and Antarctic Intermediate Water at about 27.3 mg ml^{-1}. Reid (1973) shows a vertical section of salinity at 140°W which illustrates all of these maxima. Both North Pacific Intermediate Water and Antarctic Intermediate Water have subpolar origins (Reid, 1965; Hasunuma, 1978; McCartney, 1977). On the other hand, the shallow salinity minimum of the North Pacific results from wind forcing and salinity and density distributions at the sea surface in the subtropical gyre. Reid (1973) and Tsuchiya (1982) concluded that the source of the shallow salinity minimum is the sea surface in the northeast Pacific.

The shallow salinity minimum occurs in an arc around the eastern North Pacific, as shown in Reid (1973). A notable feature of the shallow minimum is its range of density, from about 300 cl t^{-1} ($25.0\sigma_\theta$) along the eastern boundary of the Pacific to about 180 cl t^{-1} ($26.2\sigma_\theta$) on the western side of the minimum. Salinity also decreases from west to east at the minimum but isohalines and isopycnals cross on the minimum, so a simple interpretation of flow along isopycnals at the minimum is precluded.

It appears from examination of the surface salinity and density distributions and the wind forcing, presented in this paper, and from Reid's and Tsuchiya's contributions, that the shallow salinity minimum is due to the directly-ventilated, wind-driven circulation, although the sea-surface density and salinity which are advected by the wind-driven circulation are set by thermohaline processes. The shallow salinity minimum occurs on isopycnals which outcrop farthest to the north and which have the lowest salinity and highest density of outcropped isopycnals in the subtropical gyre. As water in the outcropping region is forced southward by vorticity input from Ekman pumping, it is subducted beneath higher-salinity, lower-density water to the south. Salinity is not lowest on the densest outcropped isopycnal however, so the densest subducted water in the subtropical gyre has slightly higher salinity than water at lower densities from the eastern Pacific, resulting in the necessary higher salinity water beneath the salinity minimum. Higher salinity water is also present beneath the minimum because the flow of higher-latitude water into the subtropical gyre is small underneath the

ventilated portion of the gyre (Tsuchiya, 1982). This is consistent with well-defined separation of the subtropical and subpolar circulations, a feature of several theories (e.g., Luyten *et al.*, 1983; Young and Rhines, 1982).

The central theme of this paper is how ventilation of the wind-driven subtropical gyre affects the properties there. It is worth pausing to consider what is meant by ventilation. Ventilation occurs either by Ekman pumping from the surface or by convective mixed layer processes. The difference between these two is best explained by considering some examples. In the central Labrador Sea, deep convection at very short horizontal length scales (Clarke and Gascard, 1983) effectively ventilates the North Atlantic Ocean at mid-depth (Talley and McCartney, 1982). The dominant forcing of the circulation of Labrador Sea Water is undoubtedly thermohaline. At the other end of the spectrum is the shallow salinity minimum, considered here. Whatever processes in the mixed layer set its properties and potential vorticity (convection, wind-driven stirring, or Ekman pumping into the lower part of a somewhat deep mixed layer), ventilation of the uppermost part of the subtropical North Pacific (above about 400 meters) is due to Ekman pumping; that is, the forcing which drives the circulation is Ekman pumping rather than convection. Between these two extremes is circulation of water masses such as the Subtropical Mode Water which is forced by both wind and thermohaline processes: convection is extremely important in its formation and probably also in its circulation, but it is also close enough to the sea surface to be driven by the wind. Whether it is ventilated by wind forcing is a question of whether it undergoes a process like Labrador Sea Water where it convects, sinks and spreads or remains close enough to the surface to participate in the wind-driven ventilation process.

The steady-state circulation theory of Luyten *et al.* (1983, hereafter referred to as LPS) is an excellent basis for understanding general features of the shallow salinity minimum. Luyten *et al.* distinguish between "ventilated" and unventilated regions of isopycnals which outcrop at the sea surface. Properties in ventilated zones should be nearly the same as properties where the isopycnals outcrop. Flow in unventilated regions of the isopycnals originates entirely at the western boundary and does not contact the sea surface: properties in these "shadow" zones may be governed more by the western boundary current, diffusion or thermohaline processes. Observed property distributions on isopycnals are strongly influenced by the size of western shadow zones. Since these regions were examined only cursorily by LPS, more attention is given to them here. Western shadow zones can occur in most subducted layers although LPS treated only the deepest subducted layer. The size of a western shadow zone on an isopycnal is most strongly affected by its outcrop latitude.

A modification of the LPS theory is suggested by properties of the shallow salinity minimum and wind patterns in the North Pacific. Since the wind-stress curl pattern in the North Pacific has a decided tilt, the LPS theory is considered here with such a wind field. It is emphasized that the boundary between the subtropical and subpolar gyres occurs where the Sverdrup transport function (the integrated Ekman pumping) vanishes rather than where the wind-stress curl vanishes. This is important for the salinity minimum because the maximum density at which it occurs is found at the sea-surface in winter north of the zero of wind-stress curl but south of the zero of Sverdrup forcing (integrated Ekman pumping).

In Section 2, we examine the western shadow zone when it occurs in two subducted layers of the LPS model and at the effects of layer selection on modeled circulation. The LPS model is then modified to allow for more arbitrariness and reality in the wind forcing. In Section 3, observations of salinity and potential vorticity in the North Pacific are related to general circulation theory: property distributions are strongly related to predicted ventilated and unventilated regions. It is seen that the shallow salinity minimum is a feature of the ventilated circulation and hence occurs only on ventilated isopycnals.

2. Ventilated circulation in the North Pacific

The theory of general circulation proposed by LPS concerns the wind-driven flow in isopycnal layers which outcrop at the sea surface. Luyten *et al.* assume Sverdrup dynamics throughout the ocean except in the western boundary layer which they do not treat. As in classical general circulation theories, the interior flow is assumed to be inviscid and the eddy field to be negligible. Luyten *et al.* also require that potential vorticity be conserved along flow paths in "subducted" regions in the isopycnal layers (that is, where other layers overlay the layer being considered). There are four distinct flow regimes in a given layer in the subtropical gyre—one region where it outcrops and is directly forced by Ekman pumping and three regions where it is subducted. The latter are a "ventilated" region in the center, where flow paths originate in the outcropping zone, an unventilated region along the western boundary and an unventilated region along the eastern boundary. The detailed solution actually has many more regions than these, but physically, these are the only flow regimes.

The basic assumptions of Sverdrup dynamics and potential vorticity conservation along flow trajectories are reasonable enough. Additional assumptions must also be made and at this point the modeling becomes rather more of an art. For simplicity, LPS first

assumed that flow occurs only in layers which outcrop so that the Sverdrup transport is taken up entirely in these layers. (Thus topography does not enter the problem since this circulation is confined to the upper 500 meters in the North Pacific.) Pedlosky and Young (1983) relaxed this assumption by allowing flow in regions of closed geostrophic contours in unventilated layers. Since the vertically-integrated northward flow is determined by Ekman pumping, this redistribution of flow causes the flow in ventilated layers to be reduced somewhat. However, it does not alter the qualitative aspects of the LPS solution. Second, Luyten *et al.* also assumed that there is no eastern boundary layer: therefore all moving layers but the densest have zero depth on the eastern boundary in the subtropical gyre. The depth of the densest moving layer must be specified and strongly affects the solution throughout the subtropical gyre. Pedlosky (1983) allowed an eastern boundary layer with a boundary condition of no transport through the eastern boundary and was able to construct solutions in which each layer had a nonzero depth at the eastern boundary. Inclusion of the eastern boundary layer did not affect the qualitative features of the solution in the ventilated and western unventilated region. Third, the modeler must choose the isopycnal layers for the model and their outcrops in the subtropical gyre: these choices qualitatively affect the solution. Last, LPS also assumed a wind pattern for which the zero Ekman pumping was zonal: hence the zero of Sverdrup transport coincided with the zero of Ekman pumping. This strict zonality can be relaxed, as is done in the second part of this section.

The assumptions listed to this point are sufficient to determine flow in the outcropping and ventilated regions. For the unventilated region in the west, where potential vorticity on streamlines cannot be set in an outcropping zone, LPS assumed uniform potential vorticity, citing the theory of Rhines and Young (1982) which predicts uniform potential vorticity inside closed streamlines in layers isolated from the sea surface. Ierley and Young (1983) cast some doubt on this assumption for regions where streamlines close in the western boundary layer, as they do in the western shadow zone. However, numerical model results (Holland *et al.*, 1984) and actual potential vorticity distributions in the North Pacific (Keffer, 1985) indicate that an assumption of uniform (or nearly uniform) potential vorticity in the western region is reasonable. This assumption is not pivotal to the success of the model: slight nonuniformity would probably not affect the results to any great extent.

Luyten *et al.* focused on solutions in the outcropping, ventilated and eastern unventilated zones. Their recognition of and solution in the latter were especially noteworthy. They paid less attention to the western unventilated region. In fact, their choice of isopycnal layers and outcrop latitudes reduced their western "shadow zone" to a nearly negligible part of the circulation. In the first subsection, it is shown that the western shadow zone fills almost the entire subtropical gyre if the densest outcrop in the subtropical gyre is near the zero of Sverdrup transport (and Ekman pumping, when it is strictly zonal). Also, Luyten *et al.* (1983) chose outcrops in such a way that a western shadow zone was found only in the deepest subducted layer. However, western shadow zones occur in all layers which outcrop in the northern half of the gyre. The solution with western shadow zones in two layers is given below. The size of the western shadow zone is relatively insensitive to whether such zones occur in layers above or below it and to the precise choice of layers. The size of a western shadow zone in an isopycnal layer is insensitive to the north–south extent of the outcrop. Rather, the latitude of the outcrops relative to the wind pattern is the main factor which determines the size of the western shadow zone. It is shown that as two outcrops are moved arbitrarily close together in the subtropical gyre, their western shadow zones become identical and are of limited eastward extent: hence western shadow zones in a model with a large number of ventilated layers (approaching continuous stratification) will not fill the basin entirely. A speculation on the shape of the three-dimensional western shadow zone in an ocean with continuous stratification is made.

In the second subsection, the LPS model with additional western shadow zone information is applied to three cases: simple sinusoidal Ekman pumping, zonally-dependent Ekman pumping and realistic, North Pacific Ekman pumping. In the latter two cases, the assumption of a zonally-oriented zero of Ekman pumping is relaxed; in the North Pacific (and probably in other oceans), surface isopycnals and wind patterns are not oriented zonally or parallel to each other. More difficult to relax is the assumption of zonally-oriented surface isopycnals; this is not done here. (The assumption is reasonable for the western and central North Pacific.) Also difficult is the problem when surface isopycnals intersect the zero of Sverdrup transport. This problem is skirted here by assuming that isopycnals in the subtropical gyre which intersect the zero of Sverdrup forcing follow the zero beyond the intersection and do not actually cross into the subpolar gyre.

a. Western shadow zones

Only the briefest, necessary account of the LPS theory is given here—for more detail, the reader is referred to their paper. The ocean is assumed to be divided into four layers, three of which outcrop in

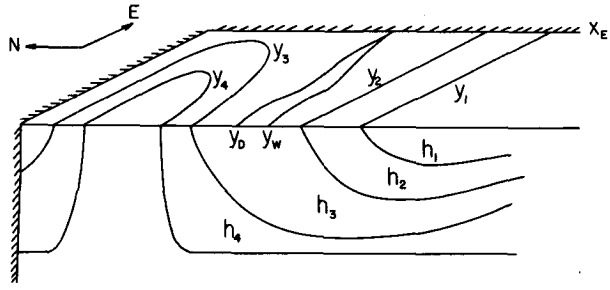

FIG. 1. Schematic of the five-layer model, after Luyten *et al.* (1983). Outcrops of the layers are indicated as y_1, y_2, y_3 and y_4. The zero of wind-stress curl is as y_w. The zero of Sverdrup forcing (D_0^2) is y_D.

the subtropical gyre, as illustrated in Fig. 1. Layer 4 is assumed to be motionless in the subtropical gyre which is defined to be the region south of the zero of Sverdrup transport. When Ekman pumping is zonal this boundary is identical to the zero of Ekman pumping.

The flow is assumed to be geostrophic, hydrostatic and incompressible. The geostrophic equations for the nth layer are

$$\left.\begin{aligned} v_n &= \frac{1}{\rho_n f}\frac{\partial \psi_n}{\partial x} \\ u_n &= -\frac{1}{\rho_n f}\frac{\partial \psi_n}{\partial y} \end{aligned}\right\}$$

where

$$\psi_n = \frac{1}{\gamma_3}\sum_{i=n}^{N}\gamma_i\Big(\sum_{j=M}^{i} h_j\Big)$$

and $\gamma_i = g(\rho_{i+1} - \rho_i)/\rho_0$ is the reduced gravity for each layer. M is the number of the top layer (the outcropping layer) and N is the number of the bottommost layer in motion so that $(N - M + 1)$ layers are in motion. In addition, v_n and h_n are the northward velocity and layer depth of the nth layer and f is the Coriolis parameter. For example, when $y_2 < y < y_w$, only layer 3 is in motion so $N = M = 3$ and $\psi_3 = \gamma_3 h_3$. Flow in layer n clearly follows contours of constant ψ_n although the velocity along those contours is not constant since f varies. Since the flow is geostrophic, hydrostatic and incompressible, the Sverdrup relation applies. For N layers, it is

$$\beta \sum_{n=1}^{N} h_n v_n = f w_E \qquad (1)$$

where w_E is the Ekman pumping velocity and $\beta = df/dy$.

A plan view of the solution with a maximum of three layers in motion in the subtropical gyre is shown in Fig. 2. This is the case solved by LPS except for three additional regions south of y_1. Luyten *et al.* found solutions in and the trajectories separating regions labeled A, B, R, M, and L in the figure. Solutions in C, D, and E are given here.

We look first at the behavior of the western shadow zone (A) in layer 3 as $y_2 \to y_w$, second at the occurrence of a shadow zone (C) in layer 2, and third, at factors which affect the size of western shadow zones. It is shown that the area of the outcropping zone does not affect the shadow zone very much.

1) WESTERN SHADOW ZONE FOR $y_1 < y < y_w$ (TWO LAYERS IN MOTION)

A western shadow zone will occur in layer 3 when it subducts beneth layer 2, south of y_2. North of y_2,

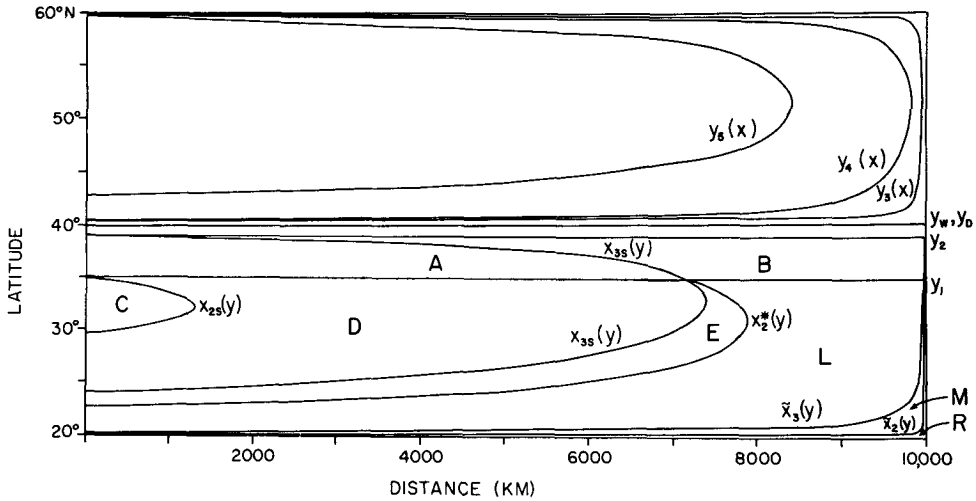

FIG. 2. Plan view of the solution with three moving layers in the subtropical gyre. Sinusoidal Ekman pumping was used. Regions A, C, and D are the western shadow zone in layer 3. Region C is the western shadow zone in layer 2. Region R is the eastern shadow zone in layer 3. Regions C, D and E are additions to the LPS solution.

layer 3 outcrops and is the only layer in motion. Luyten *et al.* showed that the solution to (1) north of y_2 is

$$h_3 = [D_0^2(x, y) + H_0^2]$$

where

$$D_0^2(x, y) = -\frac{2f^2}{\beta\gamma_3}\int_x^{x_E} w_E dx'. \quad (2)$$

Here H_0 is the depth of layer 3 at $y = y_w$ at the eastern boundary x_e.

South of y_2, where both layers 2 and 3 are in motion, western and estern shadow zones are possible where flow in the subducted layer 3 does not connect back to the outcropping zone north of y_2. In Fig. 2, the western shadow zone in layer 3 is labeled A, the ventilated region is B, and the eastern shadow zone is extremely narrow. Solutions in all three regions were found by LPS. In region B, LPS used the Sverdrup relation (1) and required that potential vorticity be conserved along flow paths in layer 3. Luyten *et al.* assumed that potential vorticity is uniform in layer 3 in the western shadow zone, A.

The western shadow zone is separated from the ventilated region by the trajectory in layer 3 emanating from the point (x_w, y_2). An implicit expression for this trajectory $x_{3s}(y)$ is LPS's (2.48):

$$D_0^2(x_{3s}, y) = D_0^2(x_w, y_2)[1 + (1 - f/f_2)^2\gamma_2/\gamma_3] + H_0^2(1 - f/f_2)^2\gamma_2/\gamma_3. \quad (3)$$

This is independent of any assumptions about potential vorticity in region A.

It is easy to see that the solution for the separating trajectory (3) has the limit

$$D_0^2(x_{3s}, y) = H_0^2(1 - f/f_2)^2\gamma_2\gamma_3^{-1}$$

as $y_2 \to y_w$ since $D_0^2(x_w, y_w) = 0$. This is precisely the trajectory which separates the eastern shadow zone from the ventilated region in layer 3 [LPS's (2.21b)]. Thus as $y_2 \to y_w$, the western shadow zone in layer 3 expands to fill the entire subtropical gyre except for the eastern shadow zone. Therefore, as is only reasonable, the entire subtropical gyre is unventilated in an isopycnal layer if the southern boundary of its outcrop coincides with the boundary between the subpolar and subtropical gyres. If potential vorticity is uniform in the western shadow zone, then we might expect to find uniform potential vorticity throughout most of the subtropical gyre on the densest isopycnal which outcrops in the subtropical gyre. [Recall however that the choice of uniform potential vorticity is an arbitrary assumption based on the theory of Rhines and Young (1982) and observational evidence of low gradients of potential vorticity in the western shadow zones.]

2) WESTERN SHADOW ZONE FOR $y < y_1$ (THREE LAYERS IN MOTION)

A western shadow zone can also occur in layer 2 where it underlies layer 1. We find solutions in this new western shadow zone in layer 2 and in the affected parts of layer 3, which are regions C, D and E of Fig. 2. Region C is the shadow zone in layer 2; D is the shadow zone in layer 3 and is a continuation of the shadow zone A found north of y_1; E is ventilated but flow in layer 2 originates in the part of the outcropping zone which overlays the shadow zone in layer 3 (Region A).

The western shadow zone in layer 3, defined by LPS's trajectory x_{3s}, is independent of the assumption of uniform potential vorticity in the shadow zone. However, shadow zones in overlying layers at least partly overlay the shadow zone in layer 3, so their size may be affected by the assumption of uniform potential vorticity in shadow zones in underlying layers. Of course the existence of shadow zones in overlying layers is independent of the assumption of uniform potential vorticity. This is quite clear in the numerical model of Cox and Bryan (1984) in which western "pools" of water which are unventilated by subduction are found in all subducted layers that they show (even though potential vorticity is not uniform in the pools). They also show a feature which will be demonstrated here: the pools are smaller, closer to the western boundary, in shallower layers.

The Sverdrup relation (1) with three layers in motion is

$$\gamma_3\frac{\partial}{\partial x}(h_1 + h_2 + h_3)^2 + \gamma_2\frac{\partial}{\partial x}(h_1 + h_2)^2 + \gamma_1\frac{\partial}{\partial x}h_1^2 = 2f^2 w_E/\beta. \quad (4)$$

In region C, we assume uniform potential vorticity in both layers 2 and 3. The potential vorticity in layer 3 is identical to its value in region A. Luyten *et al.* showed that the potential vorticity in A is f_2/H_{3w} where

$$H_{3w} = [D_0^2(x_w, y_2) + H_0^2]^{1/2}. \quad (5)$$

Thus in C,

$$\frac{f}{h_3} = \frac{f_2}{H_{3w}}. \quad (6)$$

The potential vorticity in layer 2 is

$$\frac{f}{h_2} = \frac{f_1}{H_{2w}} \quad (7)$$

where

$$H_{2w} = -\frac{f_1 H_{3w}}{f_2(1 + \gamma_2\gamma_3^{-1})} + \frac{\{(1 + \gamma_2\gamma_3^{-1})[D_0^2(x_w, y_1) + H_0^2] - \gamma_2\gamma_3^{-1}(H_{3w}f_1/f_2)^2\}^{1/2}}{(1 + \gamma_2\gamma_3^{-1})}.$$

Expressions (6) and (7) are substituted into the Sverdrup relation (4) which is then solved for h_1 yielding

$$h_1 = -(g_2h_2 + h_3)/g_1 + g_1^{-1}\{(g_2h_2 + h_3)^2 - g_1[(h_2 + h_3)^2 + \gamma_2\gamma_3^{-1}h_2^2] + g_1[D_0^2(x, y) + H_0^2]\}^{1/2}$$

where

$$g_1 = (1 + \gamma_1\gamma_3^{-1} + \gamma_2\gamma_3^{-1}) \quad \text{and} \quad g_2 = 1 + \gamma_2\gamma_3^{-1}.$$

In region D, flow in layer 2 is ventilated while flow in layer 3 is still in the western shadow zone. The Sverdrup relation (5) and equation for h_3 (6) are still true. In layer 2, potential vorticity is conserved along flow paths:

$$\frac{f}{h_2} = F_2(\psi_2). \tag{8}$$

We find F_2 by evaluating (8) at $y = y_1$ where h_1 is zero and h_2 is given by LPS's (2.50): thus

$$\left.\begin{aligned} h_2 &= \frac{f}{f_1}\,[H - g_2^{-1}(\gamma_2\gamma_3^{-1}h_3 - f_1H_{3w}/f_2)] \\ h_1 &= \left(1 - \frac{f}{f_1}\right)[H - \gamma_2\gamma_3^{-1}g_2^{-1}h_3] \end{aligned}\right\}.$$

Here $H = h_1 + h_2 + h_3$ and is determined from the Sverdrup relation to be

$$H = \left(\frac{\gamma_2}{\gamma_3}\frac{h_3}{g_2}\right) + \left[\frac{D_0^2(x, y) + H_0^3 - \gamma_2\gamma_3^{-1}g_2^{-1}h_3^2}{g_2 + \gamma_1\gamma_3^{-1}(1 - f/f_1)^2}\right]^{1/2}.$$

The trajectory x_{2s} which separates the western shadow zone and ventilated region in layer 2, that is, regions C and D, can be found from the solutions in either C or D. The trajectory is given by

$$D_0^2(x_{2s}, y) = -H_0^2 + \left[g_2 + \gamma_1\gamma_3^{-1}\left(1 - \frac{f}{f_1}\right)^2\right] \times \left[H_1 - g_2^{-1}\gamma_2\gamma_3^{-1}\left(\frac{f_1}{f_2}H_{3w}\right)\right]^2 + \gamma_2\gamma_3^{-1}g_2^{-1}\left(\frac{f}{f_2}H_{3w}\right)^2 \tag{9}$$

where

$$H_1 = H(x_w, y_1) = g_2^{-1}\gamma_2\gamma_3^{-1}\left(\frac{f_1}{f_2}H_{3w}\right) + g_2^{-1}\left\{g_2[D_0^2(x_w, y_1) + H_0^2] - \gamma_2\gamma_3^{-1}\left(\frac{f_1}{f_2}H_{3w}\right)^2\right\}^{1/2}.$$

Region E is ventilated in both layers 2 and 3 but flow paths in layer 2 originate west of (x_{3s}, y_1) in the shadow zone of layer 3: The solution differs from that of region L where layers 2 and 3 are also both ventilated. In Region E, potential vorticity is conserved along flow paths in layers 2 and 3 so $h_3 = (f/f_2)H$ where $H = (h_1 + h_2 + h_3)$ and $f/h_2 = F_3(\psi_2)$. This can be inverted for F_3 using information along $y = y_1$ west of x_{3s} to yield

$$h_2 = \frac{f}{f_1}H\left[1 - \gamma_2\gamma_3^{-1}g_2^{-1}\frac{f}{f_2}\right] - \frac{fH_{3w}}{f_2g_2}.$$

The depth of the upper layer, h_1, is of course $H - (h_2 + h_3)$. The Sverdrup relation (4) is solved for H yielding

$$H = -\frac{\gamma_1G_1fH_{3w}}{\gamma_3g_2G_2f_2} + (g_2G_2)^{-1}\left\{(\gamma_1\gamma_3^{-1}G_1)^2\left(\frac{f}{f_2}H_{3w}\right)^2 + G_2\left[g_2^2(D_0^2(x, y) + H_0^2) - \gamma_1\gamma_3^{-1}\left(\frac{f}{f_2}H_{3w}\right)^2\right]\right\}^{1/2}$$

where

$$G_1 = 1 - \frac{f}{f_1} - \frac{f}{f_2} + \frac{\gamma_2}{\gamma_3}\frac{1}{g_2}\frac{f}{f_1}\frac{f}{f_2}$$

and

$$G_2 = 1 + \frac{\gamma_2}{\gamma_3}\left(1 - \frac{f}{f_2}\right)^2 + \frac{\gamma_1}{\gamma_3}G_1^2$$

The trajectory x_{3s} which separates regions D and E is obtained from the solutions in either region and is given implicitly by

$$D_0^2(x_{3s}, y) = -H_0^2 + \left\{g_2 + \gamma_1\gamma_3^{-1}\left(1 - \frac{f}{f_1}\right)^2\right\} \times \left\{H_{3w} - g_2^{-1}\gamma_2\gamma_3^{-1}\left(\frac{fH_{3w}}{f_2}\right)\right\}^2 + g_2^{-1}\gamma_2\gamma_3^{-1}\left(\frac{fH_{3w}}{f_2}\right)^2. \tag{10}$$

The trajectory x_{3s}^* which separates E and L is obtained from the solution in either E or L [the latter is given by LPS (2.33) and (2.31)]. The implicit equation for x_{3s}^* is

$$D_0^2(x_{3s}^*, y) = -H_0^2 + F(y)H_{3w}^2\left\{\frac{1 + \gamma_2\gamma_3^{-1}(1 - f_1/f_2)}{1 + \gamma_2\gamma_3^{-1}(1 - f/f_2)}\right\}^2$$

where

$$F(y) = 1 + \frac{\gamma_2}{\gamma_3}\left(1 - \frac{f}{f_2}\right)^2 + \frac{\gamma_1}{\gamma_3}\left\{1 - \frac{f}{f_2} - \frac{f}{f_1}\left(1 - \frac{f_1}{f_2}\right) \times \left[\frac{1 + \gamma_2\gamma_3^{-1}(1 - f/f_2)}{1 + \gamma_2\gamma_3^{-1}(1 - f_1/f_2)}\right]\right\}^2.$$

3) Size of western shadow zones

What are the most important factors governing the size of the western shadow zone at a given density? Parameters which could affect its size are: number of layers above and below the layer in question, area of

the outcropping window, density difference between layers, depth of layer 3 at the eastern boundary, and latitude of the southern edge of the outcrop. We would be concerned if results depend strongly on the size of the outcrop window and number of layers since the hope is that we can learn something from a simple model with just a few layers.

To demonstrate that the number of layers chosen is not crucial to determining the eastward extent of the western shadow zone in a given layer, consider a model first with one subducted layer and then with two subducted layers. It is shown that the addition of a layer does not significantly change the western shadow zone found previously in the other subducted layer. It is also shown that the subdivision of a layer, which decreases the size of the outcropping zone as well as introducing another layer, does not significantly change the size of the western shadow zone, as long as layer densities are chosen realistically and sensibly.

Figure 3 shows the western shadow zones in the subducted layer of three models, all using sinusoidal pumping

$$w_E = W \sin[\pi y/L].$$

(This forcing was also used to produce Fig. 2.) Layer outcrops were chosen at 35°N and 39°N. Layer densities and reduced gravities for the three-layer case are listed in Table 1. The third layer, which outcrops in the subpolar gyre, was assumed to have a depth of 150 meters at the eastern boundary in accordance with Levitus' (1982) atlas. Outcrop densities in the two-layer cases are the same but reduced gravities differ because the layers are thicker and density differences are larger. (For Fig. 3a, γ_2 and γ_3 are 2.58 and 0.38, respectively. For Fig. 3b, γ_1 and γ_3 are 2.53 and 0.53.)

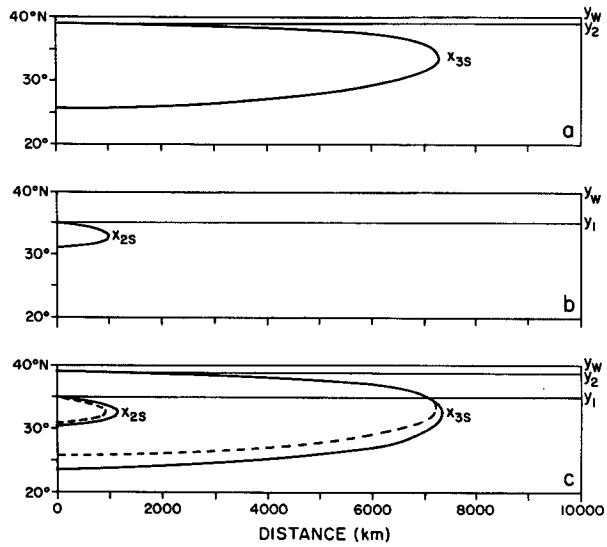

FIG. 3. Effect of additional layers on the western shadow zone: (a) Shadow zone with two moving layers and outcrop at 39°N, (b) Shadow zone with two moving layers and outcrop at 35°N and (c) Shadow zones with three moving layers and outcrops at 35°N and 39°N (solid curves). Dashed curves are from (a) and (b).

TABLE 1. Layer properties of modified LPS model with sinusoidal Ekman pumping.

n	Outcrop latitude	Interface σ_n	Average layer σ_n	γ_n
1	35°N	25.6	23.3	2.34
2	39°N	25.9	25.75	0.33
3	—	26.3	26.1	0.38
4	—	26.7	26.5	0.38
5	—	27.1	26.9	0.48
6	—	27.5	27.3	—

In Figs. 3a, b there is just one subducted layer and one western shadow zone. In Fig. 3c there are two subducted layers with the same outcrop latitudes as in Figs. 3a, b. The western shadow zones are virtually unchanged by the addition of another subducted layer. Most of the change is due to change in reduced gravity, discussed more below.

Another way of showing that the western shadow zones are little changed by the exact choice of layers to consider the fate of the western shadow zone in layer 2 as the outcrops y_1 and y_2 move close together, severely diminishing the outcrop area of layer 2. Does the shadow zone in layer 2 expand to fill the whole basin as its outcrop area decreases to zero, or is its size limited by the position of the outcrop relative to the wind pattern? Analytically, as $y_1 \rightarrow y_2$ the trajectory x_{2s} (9), which defines the western shadow zone in layer 2, is identical to x_{3s} (10), which defines the western shadow zone in underlying layer 3. Thus the shadow zone in layer 2 becomes no larger than that in layer 3 even though the outcrop area becomes very small. The trajectory x_{3s} is virtually unchanged by changes in layer 2, as was seen in the previous paragraph. This has important consequences for the conceptual expansion of the LPS model to a large number of moving layers. It means that even with oucropping zones greatly reduced in north-south extent, the area of each layer which is ventilated depends only on its outcrop latitude and not on outcrop separation.

Choice of density differences between layers can also affect the size of the western shadow zone. In the example of the previous paragraph, most of the change in shadow zone size when the number of layers is changed is due to change in reduced gravity. The larger the reduced gravity (the greater the density contrast between layers), the smaller the shadow zone. Does this mean that shadow zones fill the basin in every layer as density differences between layers are reduced and the γ_n approach zero? No, in fact the shadow zones have limited size: the limit of the separating trajectories (3) and (9) as $\gamma_n \rightarrow 0$ such that γ_n/γ_{n+1} is constant is

$$D_0^2(x_{3s}, y) \rightarrow D_0^2(x_w, y_2)\left[1 + \left(1 - \frac{f}{f_2}\right)^2 \gamma_2\gamma_3^{-1}\right]$$

$$D_0^2(x_{2s}, y) \rightarrow D_0^2(x_w, y_2)\left[1 + \left(1 - \frac{f}{f_1}\right)^2 \gamma_1\gamma_3^{-1}g_2^{-1}\right]$$

$$+ D_0^2(x_w, y_2)\frac{\gamma_2}{\gamma_3 g_2}\left\{\left(\frac{f}{f_2}\right)^2 - \left(\frac{f_1}{f_2}\right)^2 \times \left[1 + \left(1 - \frac{f}{f_1}\right)^2 \gamma_1\gamma_3^{-1}g_2^{-1}\right]\right\}.$$

A feature of these limits on western shadow zone sizes is that they are independent of H_0, the assumed depth of the third layer at the eastern boundary. Several trials of the model with nonzero γ_n and widely varying H_0 showed that western shadow zone sites are relatively independent of H_0. (On the other hand, the width of the eastern shadow zone depends strongly on H_0.)

Do western shadow zones occur in all subducted layers in the subtropical gyre? No, they do not occur when the southern edge of the outcrop zone is too far south of the middle of the gyre, as defined by the maximum of D_0^2, the Sverdrup forcing. It is easy to show analytically that there is no western shadow zone in layer 3 if the southern edge of its outcrop coincides with the latitude where D_0^2 is maximum at the western boundary: in this case the trajectory x_{3s}, which defines the western shadow zone in layer 3, goes due south at the western boundary. When y_2 is even farther south, x_{3s} goes southwest at the western boundary; hence there is no western shadow zone. When there are two subducted layers and layer 3 outcrops in the northern part of the gyre and has a western shadow zone, it is much more difficult to show analytically that the western shadow zone in layer 2 (defined by x_{2s}) disappears when the outcrop y_1 is at or slightly south of the maximum of D_0^2. In model runs however, the western shadow zone in layer 2 disappears when y_1 is south of the gyre center. Thus we surmise that western shadow zones occur predominantly on isopycnals which outcrop in the northern half of the gyre.

In order to compare theory and observations, we can speculate about the shape of the western shadow zone in a model with a large number of layers which outcrop at closely-spaced intervals in the subtropical gyre. We saw that a single additional layer which has its own western shadow zone does not affect the western shadow zone in the original, subducted layer. We saw that reduced gravities, the γ_n, do not greatly affect the western shadow zone. We saw that western shadow zones are not much affected by the proximity of outcrops and hence by the total outcropping area. Thus we speculate that in a model with a large number of thin layers, the three-dimensional western shadow zone would be a smooth, inverted, skewed bowl. It is relatively easy to picture the three-dimensional region of uniform potential vorticity: it fills almost the entire basin at the highest ventilated density, is increasingly limited to the west as density decreases, and disappears for isopycnals which outcrop in the southern half of the gyre.

The observed potential vorticity distribution in the North Pacific, presented in Section 3, closely resembles this schematic potential vorticity distribution. We also see in Section 3 that western shadow zones strongly affect salinity distributions on ventilated isopycnals in the North Pacific and that the shallow salinity minimum can be attributed to the ventilated circulation.

b. *Models of North Pacific circulation*

The examples of previous sections use sinusoidal Ekman pumping and zonal isopycnal outcrops. As a second problem, wind stress curl with zonal dependence is chosen:

$$w_E = W \sin[\pi(y + ax)/L]. \quad (11)$$

Figure 4 shows the Ekman pumping and Sverdrup forcing D_0^2. (Notice that there is a region in the west where this is positive w_E and upwelling but where D_0^2 is negative, so that flow is in the subtropical gyre there.) The layers and outcrops selected are the same as in the first example except that outcrops are not allowed to cross the zero of Sverdrup forcing D_0^2. In order for an outcrop to cross from the subtropical to the subpolar gyre, there must be cross-gyre baroclinic transport (with no net barotropic transport of course). This problem is unsolved as stated here, although Pedlosky (1984) found solutions with cross-gyre baroclinic transport divided between the surface and a completely submerged layer.

Trajectories in all layers are shown in Fig. 5. The outcrop at 39°N crosses the zero of w_E, west of which barotropic flow is northeastward. In layer 3, water flows out of the western boundary south of the outcrop, emerges into an outcropping zone and then is subducted. The western shadow zone in layer 3 is now defined by the trajectory which grazes the intersection of the outcrop and the zerro of w_E. Although there is technically nothing wrong with this solution of the steady-state model, it does pose an intuitive difficulty since flow trajectories in layer 3 between the western boundary and the outcropping zone are now determined by processes upstream in the outcropping zone. However, since the flow is steady, it presumably would have equilibrated over time, with proper adjustments in the western boundary layer, to yield this solution. Whether or not such a steady-state solution would actually obtain is not answered. The eastern shadow zone is virtully unchanged from the simple sinusoidal case of the previous paragraph. Flow in layer 1 has a peculiar glitch where flow paths cross region E (Fig. 2). This is a region which is

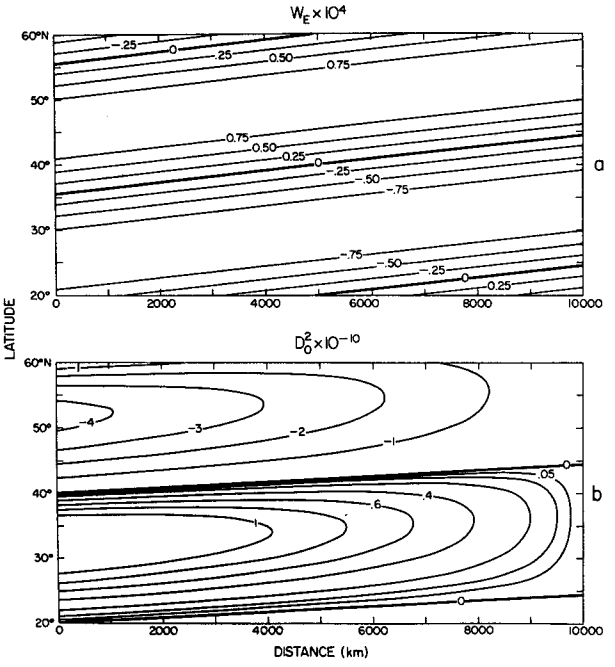

FIG. 4. (a) Ekman vertical velocity w_E (11), and (b) associated Sverdrup forcing D_0^2.

ventilated in all three layers but where flow paths in layer 2 originated above the shadow zone of layer 3. It is not clear how this would generalize in a model with many layers: could such a feature be related to the Subtropical Countercurrent (Cushman-Roisin, 1984)?

We now apply more realistic winds to a more realistic model of the stratified ocean. Figure 6 shows Ekman pumping w_E and Sverdrup forcing D_0^2 derived from the annually-averaged wind stresses and curls of Han and Lee (1981), whose source was National Climatic Center data. Notice how much more zonal D_0^2 is than the Ekman pumping because of integration. Figure 7 shows salinity and density σ_θ at the surface in late winter from Levitus (1982). It is quite clear from Figs. 6 and 7 that sea surface isopycnals cross y_D: this would also be true if late winter rather than annual winds were used. This crossing is not modeled here. Layer choices are listed in Table 2; the outcrops $26.0\sigma_\theta$ and $25.6\sigma_\theta$ are chosen at 40 and 35°N when they lie south of y_D. Flow regimes in each layer are shown in Fig. 8, corresponding to regions shown in Fig. 2. Notice how large the western shadow zone is in layer 3, because of the close proximity of y_2 to y_D.

The only real change in the basic LPS solution when nonzonal forcing is used is occurrence of upward Ekman pumping in the subtropical gyre. Likewise there could be downwelling in portions of the subpolar gyre. An aspect of the data which was not modeled here is the crossing of sea surface isopycnals and y_D. It may be possible to model this crossing with a steady-state model if baroclinic flow across y_D is permitted so that there is flow in more than one layer in the subpolar gyre. Seasonal forcing may also account for the apparent crossing of surface isopycnals and y_D. In Parson's (1969) model, an outcrop crosses from the subtropical to the subpolar gyre because of nonzero Ekman flow at y_D which is balanced by geostrophic flow across y_D. The net flow is rather small, on the order of 3×10^6 m^3 s^{-1}, but it allows the outcrop to cross the gyre boundary.

3. Salinity and potential vorticity in the ventilated North Pacific

The existence of a shallow salinity minimum in the subtropical North Pacific is consistent with the ventilated circulation model of LPS, given realistic surface density and salinity distributions. In the first part of this section it is shown how a shallow salinity minimum can arise in the circulation model. In the second part, salinity and potential vorticity are examined on several isopycnals which outcrop in the North Pacific Subtropical gyre: they are consistent with model predictions of where ventilated and unventilated regions occur.

a. Shallow salinity minimum

The shallow salinity minimum occurs only at densities which outcrop in the subtropical gyre, based on sea-surface density (Fig. 7b), Sverdrup forcing (Fig. 6b) and Reid's (1973) map of the feature's density. The minimum therefore is linked with ventilation of the gyre. Of course there are both ventilated and unventilated regions on isopycnals which outcrop in the subtropical gyre: since the shallow salinity

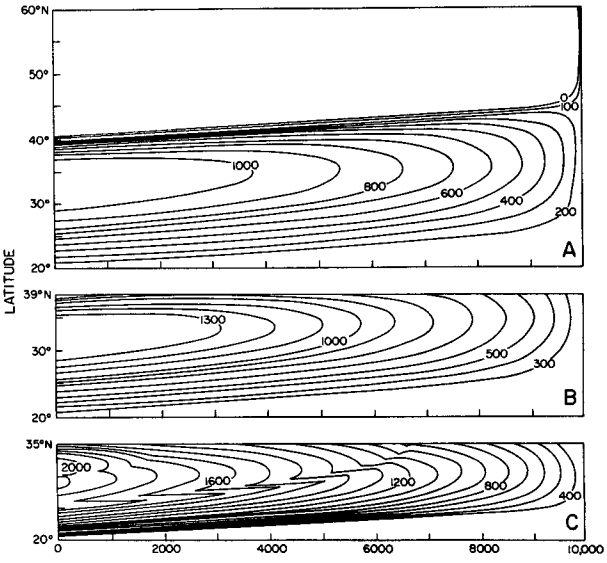

FIG. 5. Flow paths for the forcing of Figure 4 in (a) layer 3, (b) layer 2, and (c) layer 1.

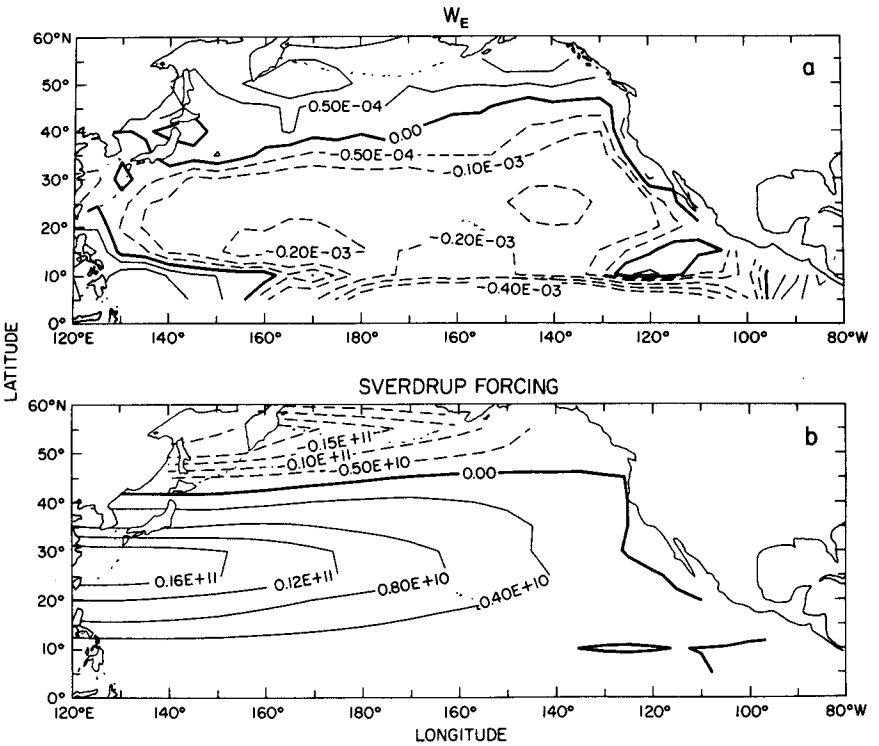

FIG. 6. (a) Ekman pumping velocity w_E derived from annual-average wind-stress and wind-stress curl of Han and Lee (1981). (b) Associated Sverdrup forcing D_0^2.

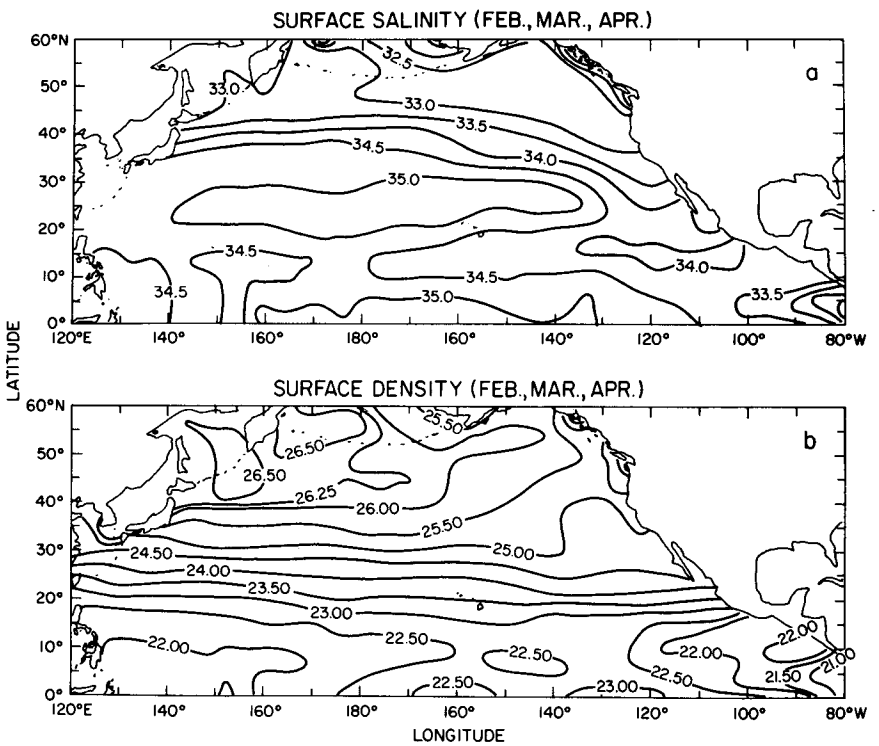

FIG. 7. (a) Average sea-surface salinity and (b) sea-surface density for February, March and April from Levitus (1982).

TABLE 2. Layer properties for North Pacific winds.

n	Outcrop latitude	Interface σ_n	Average layer σ_n	γ_n
1	35°N	25.50	24.00	1.67
2	40°N	26.00	25.75	0.43
3	—	26.40	26.20	0.38
4	—	26.80	26.60	—

minimum occurs around the eastern periphery of the gyre, which is ventilated in the model, the minimum is probably linked to ventilation. Production of the salinity minimum using the circulation model and realistic winds and surface density and salinity distributions is illustrated in a series of easy steps.

First consider an ocean with three outcropped layers in the subtropical gyre. Suppose the salinity at the outcrop of the middle layer is lower than at the outcrops of the other two layers. The first model of Section 2 with zonal, sinusoidal Ekman pumping, is used. There will be a salinity minimum in region E of Fig. 2 where layer 2 is ventilated with low salinity water. Whether or not there is a salinity minimum to the west in the shadow zone in layer 2 depends on whether the salinity there achieves its values through horizontal or vertical mixing or some thermohaline process. This simplistic model of sea-surface salinity is not very relevant to the North Pacific although it shows clearly how a salinity minimum can arise.

More relevant to the Pacific is a similar model with salinity which varies along the outcrops. The third model of the previous section with realistic winds and surface density was used. Salinity along outcrops, whose densities are 25.5 and 26.0σ_θ, was chosen from Levitus' surface salinity and density in winter (Fig. 7). Salinity decreases toward the east along the outcrops. The actual outcrops cross into the subpolar gyre: since the densest isopycnals cross farther to the west than lighter ones and since salinity decreases to the east at the surface, the lowest salinity at 25.5σ_θ is lower than the lowest salinity at 26.0σ_θ.

Figures 9a and b show the density and salinity of the modeled salinity minimum, obtained by plotting trajectories from each isohaline at the outcrops and locally determining in which layer the salinity minimum occurred. It was assumed that salinity is conserved along flow paths. It was also assumed that salinity in the top and bottom layers (1 and 4) is higher than salinities shown in Fig. 9b. (Levitus' data shows an average salinity of 34.1‰ at 26.6σ_θ, the density of layer 4; the salinity of layer 1 is not uniformly high, but since salinity is higher to the south at the surface and since layer 1 is assumed to represent all surface layers above layer 2, at 25.75σ_θ, the assumption of higher salinity in layer 1 is justified.)

The predicted salinity minimum is in layer 3 in the west and layer 2 in the east. The salinity varies from 34 to less than 33‰. Note that isopycnals and isohalines intersect on the salinity minimum surface even though no mixing is allowed in the model. This is possible since flow is directed along isopycnals rather than along the salinity minimum and since there are salinity gradients at the isopycnals' outcrops. The salinity minimum is found at a given density and salinity when it happens that the water above and below it, whose surface origins were at different places, has higher salinity. The most unrealistic feature of the modeled salinity minimum is the low value of salinity predicted on the southern side of the gyre. Mixing clearly has some effect: if salinity were exactly conserved along flow paths, there would be large north–south gradients of salinity on the southern flank of the gyre. Isopycnal mixing would undoubtedly soften the contrast.

It is assumed that continuous ocean stratification can be modeled with many layers. Details of the LPS solution will vary when the upper, ventilated ocean is split into more layers but the general character of

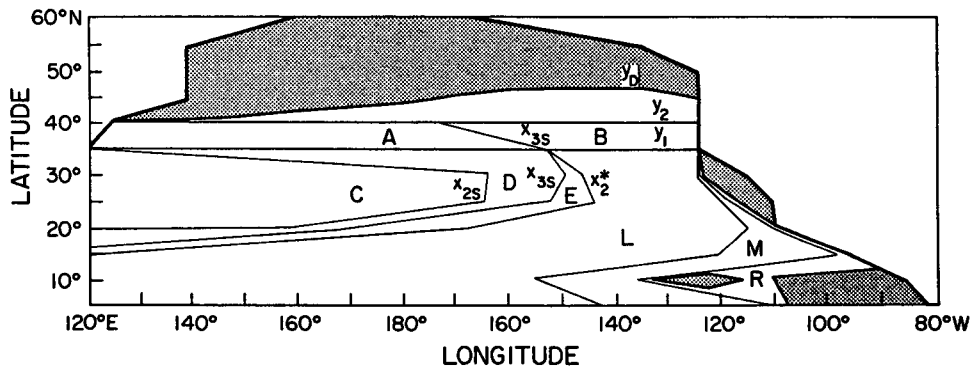

FIG. 8. Flow regions in the subtropical gyre of the modified LPS model (corresponding to those of Fig. 2) using realistic forcing from Fig. 6. Outcrops were selected based on the actual sea-surface density in Fig. 7(a). Shaded regions indicate negative D_0^2.

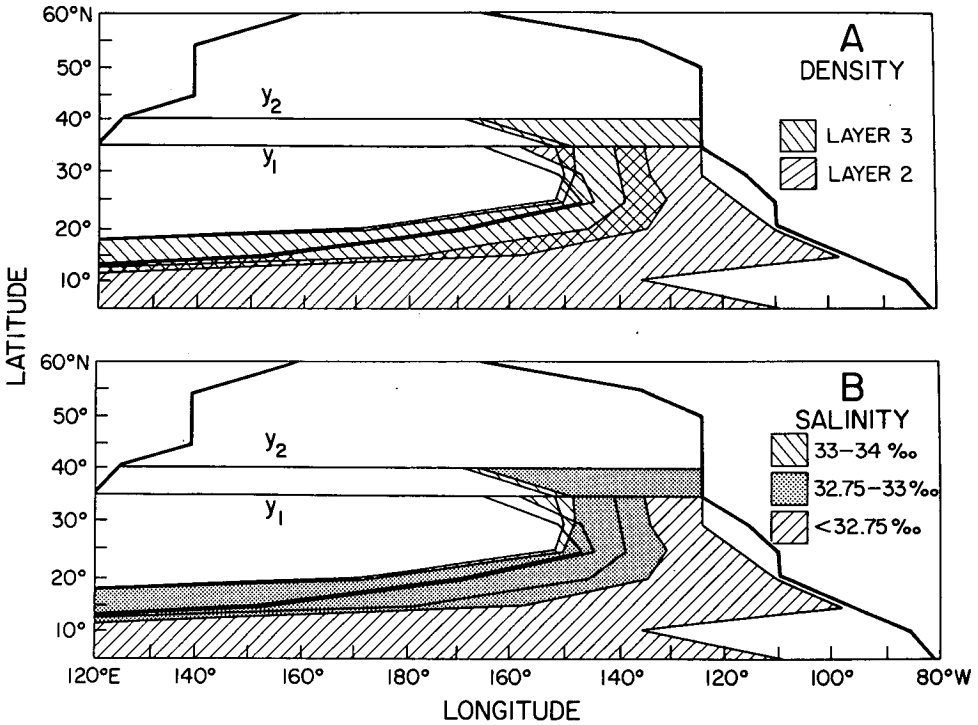

FIG. 9. (a) Density and (b) salinity at the shallow salinity minimum from the modified LPS model, using realistic winds and sea-surface density and salinity, all shown in the previous figures. The light, nonzonal lines are trajectories in layers 2 and 3. If salinity is conserved along flow paths, the trajectories correspond to isohalines. The intersection of the trajectories with the outcrops was based on sea-surface salinity and density in Fig. 7. Because of discrete layer depths and salinity values, there are regions where the minimum occurs in both layers 2 and 3 (when the salinity in layers 2 and 3 is the same but less than that in layers 1 and 4).

the flow will not. The shallow salinity minimum should occur along the north, east and south sides of the gyre since these are the only ventilated regions. In fact, the observed shallow salinity minimum is found only in these regions (Reid, 1973).

The exact density of the shallow salinity minimum depends entirely on trajectories in all layers: that is, what salinity water has been brought in from the outcrop region. The greatest density the shallow salinity minimum can occur at will be near the maximum density outcropped in the subtropical gyre. Because the density of the local shallow salinity minimum depends on trajectories in all layers, it is clear that the minimum does not originate at one given place: flow is not continuous along the minimum except perhaps very locally. The density of the observed minimum varies from high on the western, inside edge to low on the eastern, outside edge because of the salinity distribution at outcrops. Consider the lowest surface salinity at $26.0\sigma_\theta$, which is approximately 33.0‰. The same low salinity occurs at the outcrop of $25.6\sigma_\theta$ farther to the east. Immediately south and east of the $26.0\sigma_\theta$ outcrop, the minimum will occur at $26.0\sigma_\theta$ where it underlies higher salinity water at $25.6\sigma_\theta$. Even farther to the east however, the salinity at the $25.6\sigma_\theta$ outcrop is about 32.75‰, so the shallow salinity minimum will shift to the $25.6\sigma_\theta$ surface. Thus density and salinity at the minimum decrease to the east. Note that isopycnals and isohalines at the minimum do not necessarily have to coincide since there is no reason to expect flow, except locally, along the shallow salinity minimum.

It has been assumed in the model that potential vorticity, density and salinity are conserved along flow paths: this is a reasonable conjecture for a model but is it really true? In the next subsection, salinity and potential vorticity at relevant densities in the North Pacific are shown and compared with the model.

b. Salinity and potential vorticity distributions on isopycnals

Temperature and salinity values at 33 standard depths from Levitus' (1982) averaged and objectively-mapped hydrographic data were used to examine properties on density surfaces in the North Pacific. Data were interpolated to standard density (σ_θ) levels separated by $0.05\sigma_\theta$ using the method outlined in Talley and McCartney (1982) throughout this paper and in Levitus (1982), the old equation of state was used. Potential vorticity $(f/\rho)\partial\rho/\partial z$ was calculated by recomputing the density difference between two adjacent levels at the pressure midway between the

two levels. The approximate potential vorticity is calculated from the difference in the recomputed densities and the depth between adjacent σ_θ levels. This is identical to the procedure often used to calculate Brunt-Väisälä frequency.

The Levitus data set has the benefit of being less contaminated by time-dependent, small-scale features than individual stations. However, features of medium-size in the horizontal may be somewhat degraded by the averaging. The shallow salinity minimum is resolved by Levitus' data and its density, salinity, and depth ranges coincide reasonably well with Reid's (1973) description based on individual sections.

Figure 10 shows salinity at 25.5, 26.0 and 26.8σ_θ in the North Pacific. The two lighter isopycnals intersect the sea surface in the subtropical gyre in winter and are ventilated. They are the upper interfaces of layers 2 and 3 in the model. At both 25.5 and 26.0σ_θ, there is a large region of low salinity gradient to the west with higher gradients to the north, east and south. Keffer (1985) shows potential vorticity for the interval 26.05–26.25σ_θ, which is also ventilated in the subtropical gyre: similarly low gradients of potential vorticity occur in the west with higher gradients around the edges.

Figure 11 shows potential vorticity at 25.525, 26.025 and 26.825σ_θ, calculated as explained above. At 25.525 and 26.025σ_θ, the western shadow zones are well defined by low gradient regions, with an increase in shadow zone size with depth.

The isopycnal 26.8σ_θ is not ventilated anywhere in the North Pacific: this is the density of the main salinity minimum (which is separated vertically from the shallow salinity minimum by waters of density 26.25–26.8σ_θ which outcrop in the subpolar gyre). Potential vorticity and salinity have only weak meridional gradients at 26.8σ_θ, markedly different from less dense, ventilated levels.

Western regions of low gradients of salinity and potential vorticity coincide with predicted, unventilated regions on the isopycnals. In the previous subsection, realistic winds were applied to an ocean with three layers which are ventilated in the subtropical gyre. The western shadow zones in the lower two ventilated layers were found. It was shown in the previous, more theoretical section, that the extent of these shadow zones was insensitive to the number of moving (two or three) layers. Western shadow zones for the modeled ocean using the Han and Lee winds and Levitus surface density are superimposed on the salinity distributions in Fig. 10. The coincidence of the low-gradient regions in salinity and the shadow zones is remarkable and suggests that the model successfully predicts regions of ventilated and unventilated wind-driven circulation. Ventilation of the western region by thermohaline forcing is not precluded (but is not included in the model): the Subtropical Mode Waters of the western Pacific and Atlantic (Masuzawa, 1969; Worthington, 1959) are ventilated in late winter by convection, rather than by wind driving.

Regions of higher gradients in salinity and potential vorticity are identified as ventilated zones. According to the LPS solutions of the previous section, flow should be continuous around the gyre from the outcropping zone to the western boundary. An assumption of the model was that potential vorticity and density are conserved along flow paths. In Fig. 10 and Keffer's potential vorticity maps, it appears that salinity and potential vorticity are not conserved along flow paths—in fact, dynamic topography (Tsuchiya, 1982) indicates that it is more correct to infer flow paths from tongues of low salinity extending around the gyre than from isohalines. Thus there must be mixing along flow paths. However, because of the success of the inviscid model in predicting trajectories, regions of low gradients in salinity and potential vorticity, and the existence of the shallow salinity minimum, it may be that mixing affects the model only at a higher order.

Other water properties show the same patterns as salinity and potential vorticity. Tsuchiya (1982) presented oxygen, nitrate, phosphate and silica on an isopycnal which is nearly the same as $\sigma_\theta = 25.5$. The latter three properties look very much like salinity and potential vorticity. Fine *et al.* (1981) present tritium distributions at potential densities σ_θ of 23.9, 26.02 and 26.81. Although their data are sparse, the general features are similar to the other tracers. Thus a large suite of tracers confirm that there is surface ventilation of the subtropical gyre.

One might be tempted to conclude from the contrast in property gradients between the western shadow region and the ventilated region that there is a difference in mixing rates in the two regions. While there may be a difference, it cannot be estimated from the information given here. Mixing is indicated in both regions: the main reason for differences in properties is the difference in source waters for the two regions. In the western shadow zone, properties are determined by sporadic overturning at the sea surface in winter which probably has similar characteristics year after year (Talley and Raymer, 1982) and by horizontal or vertical diffusion. In ventilated regions, properties are determined by the wide range of properties at isopycnal outcrops and by mixing which produces tongues of salinity and potential vorticity along or crossing flow paths.

Vertical sections of potential vorticity along 140 and 160°E are shown in Fig. 12. The isopycnal 26.25σ_θ is the densest isopycnal which outcrops in the subtropical gyre: all ventilation by wind driving occurs at lighter densities. In Section 2, a speculation was made about the shape of the western shadow zone which agrees well with the potential vorticity distribution above 26.25σ_θ in Fig. 11. Moreover, the western shadow zone is more strongly restricted to

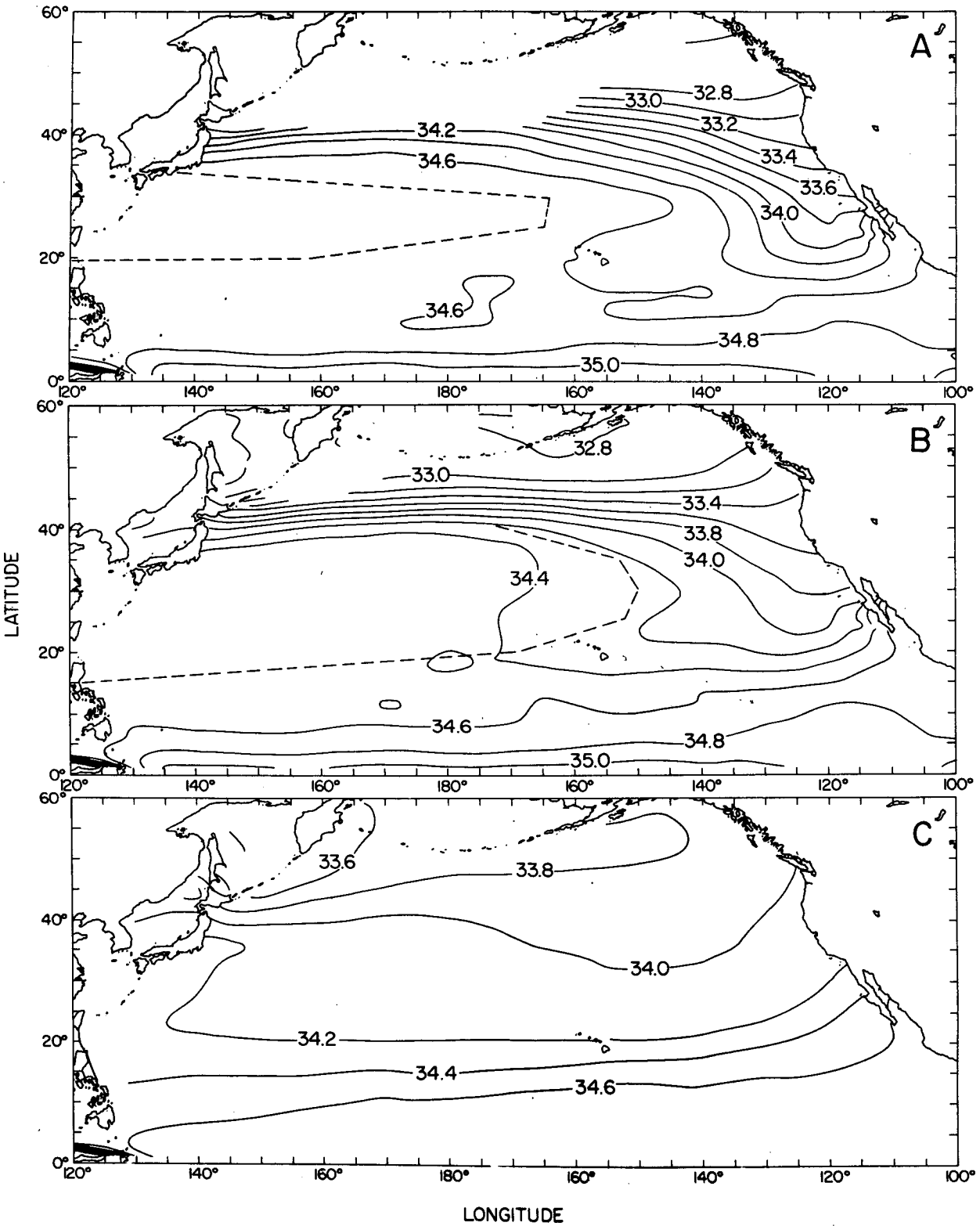

FIG. 10. Salinity at (a) $25.5\sigma_\theta$, (b) $26.0\sigma_\theta$ and (c) $26.8\sigma_\theta$ based on averaged NODC data from Levitus (1982). Contours in (a) and (b) terminate at the northernmost extent of each density surface in the annual-averaged data sets. (Winter outcrops shown in Fig. 7 occur farther to the south.) Dashed lines are the western shadow zones from Fig. 8.

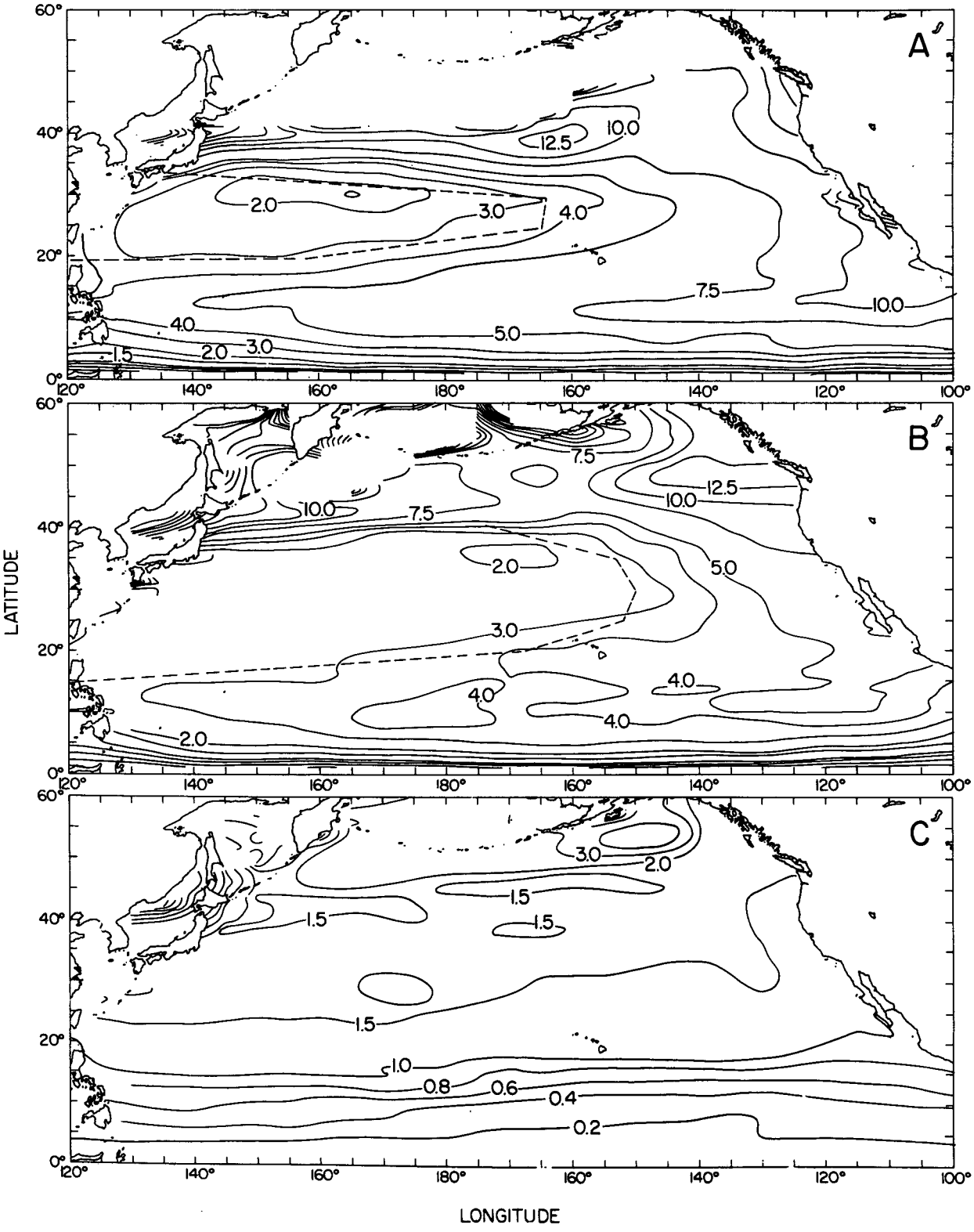

FIG. 11. Potential vorticity at (a) $25.525\sigma_\theta$, (b) $26.025\sigma_\theta$ and (c) $26.825\sigma_\theta$ based on averaged NODC data from Levitus (1982).

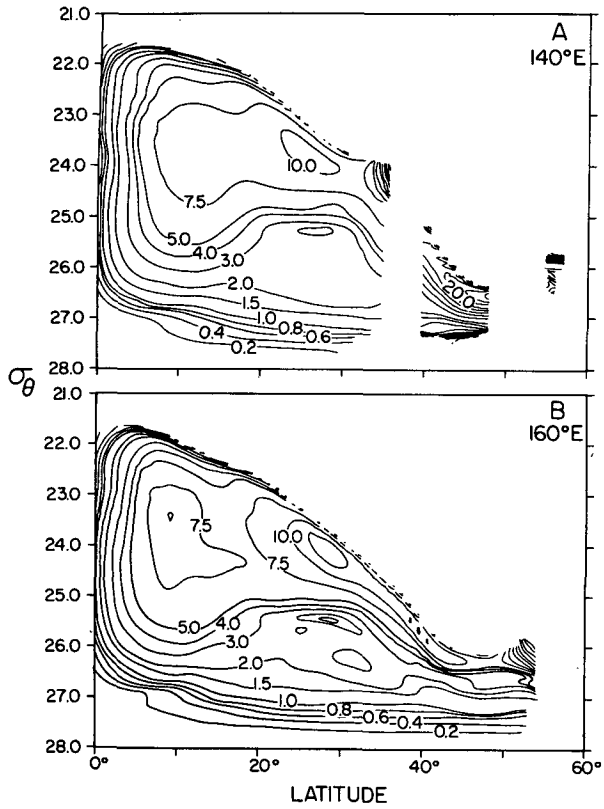

FIG. 12. Potential vorticity as a function of density and latitude at (a) 140°E and (b) 160°E. Water less dense than $26.25\sigma_\theta$ outcrops in the subtropical gyre in winter. From Fig. 6b, the gyre boundary is at about 42°N on both sections. Regions with very low north–south gradients of potential vorticity above $26.25\sigma_\theta$ presumably correspond to western shadow zones. Below $26.25\sigma_\theta$ in the subtropical gyre flow is unventilated: regions of nearly constant potential vorticity presumably correspond with those predicted by Young and Rhines (1982). Above $26.25\sigma_\theta$, potential vorticity is minimum where it is uniform. Below $26.25\sigma_\theta$, potential vorticity is maximum where it is uniform.

the western boundary at lower densities, which also corroborates the theory of Section 2. Below $26.25\sigma_\theta$ in the subtropical gyre, there are also low gradients of potential vorticity. This region can be identified with Rhines and Young's (1982) region of homogenized potential vorticity and has been noted by Keffer (1985) and Holland *et al.* (1984).

4. Conclusion

The shallow salinity minimum has been shown to be a feature of the wind-driven, ventilated circulation in the subtropical gyre. It arises "accidentally" as a result of sea-surface salinity and density in winter. It marks fairly clearly the greatest density that is ventilated in the subtropical gyre, although this too is a coincidence of a general decrease in sea-surface salinity to the north. (On the other hand, it does not indicate the full region of ventilation.) The density and salinity of the shallow salinity minimum vary as a result of the flow pattern established by the winds and variation in sea-surface density and salinity. Thus the shallow salinity minimum does not mark a flow path: it is not necessary to invoke mixing to account for variation in properties at the salinity minimum (although mixing is needed to account for the actual salinity at the minimum). While the source of low salinity water is undoubtedly the northeastern Pacific, it is not necessary to look farther than the northern regions of the subtropical gyre, which extends to 45°N off the North American coast. It is not necessary to invoke geostrophic transport between the subpolar and subtropical gyres to produce the shallow salinity minimum except perhaps to balance Ekman layer transport which may maintain low salinity in the northeastern subtropical gyre.

The shallow salinity minimum was discussed in terms of a steady-state general circulation model. However, the actual situation at the sea surface in late winter is much more complicated than the smooth density and salinity distributions assumed here. The "formation" region for the shallow salinity minimum is roughly between 28 and 45°N, within a broad region of frontal activity in the upper 100 meters (Roden, 1980; Niiler and Reynolds, 1984). Interleaving and occasional multiple salinity minima in the mixed layer are characteristic of this area. Moreover the shallow salinity minimum appears to have considerable small-scale horizontal variability and usually appears as a distinct intrusion (Hayward and McGowan, 1981; Kenyon, 1978). It is also nearly coincident with an oxygen maximum (Kenyon, 1978). Thus large-scale features of the salinity minimum are well described by the general circulation theory but close examination of the minimum reveals variability and structure which are not part of the steady-state model. The connection between the mixed layer with its small-scale, intense, transient deformations and the general circulation is not understood, although the water that makes up the salinity minimum may arise at these fronts before being "injected" into and becoming a signature of the general circulation of the underlying waters.

Attention was given to the western, unventilated regions of isopycnal layers in the Luyten *et al.* (1983) model. Solutions were derived for the case when such a western "shadow zone" occurs in two subducted layers. It was seen that the eastward extent of the western shadow zones is relatively insensitive to the number of layers, north–south extent of the layer's outcrop, and specific choice of layers (as long as the choice is realistic).

It was seen that if the southern edge of a layer's outcrop coincides with the boundary between the subtropical and subpolar gyres (defined by the zero of the zonal integral of Ekman vertical velocity), then that layer is totally unventilated in the subtropical gyre. The western and eastern shadow zones completely fill the gyre at that isopycnal.

On the other hand, it was shown that the western

shadow zone in any other layer which outcrops in the subtropical gyre is of limited eastward extent no matter how small the area of its outcrop: there is always a ventilated region on any isopycnal which outcrops within the subtropical gyre, and it is never smaller than the ventilated region of the underlying isopycnal.

It was seen empirically from the model with three moving layers in the subtropical gyre that isopycnals which outcrop south of the gyre center, where Sverdrup transport is maximum, are fully ventilated (they have no western shadow zones).

It was seen that the eastern shadow zone is extremely small for parameters relevant to the North Pacific; the width of this zone depends very strongly on H_0 which is the depth on the eastern boundary of the densest ventilated layer in the subtropical gyre. Because the North Pacific is extremely well-stratified in comparison with the North Atlantic, H_0 in the Pacific is rather small (150 meters as opposed to 800 meters) and the North Pacific's eastern shadow zone is of very limited extent. An observed feature of the North Pacific, which at first glance might be identified with an eastern shadow zone, is a bulge in properties at 10–20°N, 110–130°W: this feature however results from upward Ekman pumping (Hofmann *et al.*, 1981).

The model does not include mixing and therefore cannot exactly produce salinity and potential vorticity on isopycnals or the shallow salinity minimum's properties. These properties appear more as elongated tongues around the eastern side of the gyre: the tongues follow dynamic topography somewhat so it appears that flow is better traced along the tongues than around them. (Cox and Bryan, 1984, show streamlines crossing tongues obliquely.) The model however is extremely successful at predicting boundaries of regions off low property gradients (western shadow zones): thus it appears that mixing does not affect model dynamics at lowest order in ventilated regions.

Acknowledgments. I thank Roland de Szoeke and Jim Richman for providing me with the opportunity to do this study and for their input and encouragement. Discussions with J. Reid were helpful. This work was started with funding from NSF OCE8117700, NSF OCE8316930 and ONR N00014-79-C-0004 to Oregon State University and was completed while the author was supported by a Mellon Foundation fellowship at SIO.

REFERENCES

Clarke, R. A., and J. C. Gascard, 1983: The formation of Labrador Sea Water. Part II: Mesoscale and smaller-scale processes. *J. Phys. Oceanogr.*, **13**, 1779–1797.

Cox, M. D., and K. Bryan, 1984: A numerical model of the ventilated thermocline. *J. Phys. Oceanogr.*, **14**, 674–687.

Cushman-Roisin, B., 1984: On the maintenance of the subtropical front and its associated countercurrent. *J. Phys. Oceanogr.*, **14**, 1179–1190.

Fine, R. A., J. L. Reid and H. G. Ostlund, 1981: Circulation of tritrium in the Pacific Ocean. *J. Phys. Oceanogr.*, **11**, 3–14.

Han, Y.-J., and S.-W. Lee, 1981: A new analysis of monthly mean wind stress over the global ocean. Climatic Research Institute, Rep. No. 26, Oregon State University, 148 pp.

Hasunuma, K., 1978: Formation of the intermediate salinity minimum in the northwestern Pacific Ocean. *Bull. Ocean. Res. Inst., Univ. Tokyo*, **9**, 47 pp.

Hayward, T. L., and J. A. McGowan, 1981: The shallow salinity minimum and variance maximum in the central North Pacific. *Deep-Sea Res.*, **28**, 1131–1146.

Hofmann, E. E., A. J. Busalucchi and J. J. O'Brien, 1981: Wind generation of the Costa Rica Dome. *Science*, **214**, 552–554.

Holland, W. R., T. Keffer and P. B. Rhines, 1984: Dynamics of the general circulation: the potential vorticity field. *Nature*, **308**, 698–705.

Ierley, G. R., and W. R. Young, 1983: Can the western boundary layer affect the potential vorticity distribution in the Sverdrup interior of a wind gyre? *J. Phys. Oceanogr.*, **13**, 1753–1763.

Keffer, T., 1985: The ventilation of the world's oceans: maps of the potential vorticity field. *J. Phys. Oceanogr.*, **15**, (in press).

Kenyon, K. E., 1978: The shallow salinity minimum of the eastern North Pacific in winter. *J. Phys. Oceanogr.*, **8**, 1061–1069.

Levitus, S., 1982: *Climatological Atlas of the World Ocean.* NOAA Prof. Paper 13, 173 pp.

Luyten, J. R., J. Pedlosky and H. Stommel, 1983: The ventilated thermocline. *J. Phys. Oceanogr.*, **13**, 292–309.

Masuzawa, J., 1969: Subtropical mode water. *Deep-Sea Res.*, **16**, 463–472.

McCartney, M. S., 1977: Subantarctic mode water. *A Voyage of Discovery*, Pergamon, 103–119.

Niiler, P. P., and R. W. Reynolds, 1984: The three-dimensional circulation near the eastern North Pacific subtropical front. *J. Phys. Oceanogr.*, **14**, 217–230.

Parsons, A. T., 1969: A two-layer model of Gulf Stream separation. *J. Fluid Mech.*, **39**, 511–528.

Pedlosky, J., 1983: Eastern boundary ventilation and the structure of the thermocline. *J. Phys. Oceanogr.*, **13**, 2038–2044.

——, 1984: Cross-gyre ventilation of the subtropical gyre: an internal mode in the ventilated thermocline. *J. Phys. Oceanogr.*, **14**, 1172–1178.

——, and W. R. Young, 1983: Ventilation, potential vorticity homogenization and the structure of the ocean circulation. *J. Phys. Oceanogr.*, **13**, 2020–2037.

Reid, J. L., Jr., 1965: Intermediate waters of the Pacific ocean. *The Johns Hopkins Oceanographic Studies*, Vol. 2, 85 pp.

——, 1973: The shallow salinity minimum of the Pacific Ocean. *Deep-Sea Res.*, **20**, 51–68.

Rhines, P. B., and W. R. Young, 1982: A theory of the wind-driven circulation 1. Mid-Ocean Gyres. *J. Mar. Res.*, **40**(Suppl.), 559–596.

Roden, G. I., 1980: On the subtropical frontal zone north of Hawaii during winter. *J. Phys. Oceanogr.*, **10**, 342–362.

Talley, L. D., and M. S. McCartney, 1982: Distribution and circulation of Labrador Sea Water. *J. Phys. Oceanogr.*, **12**, 1189–1205.

——, and M. E. Raymer, 1982: Eighteen degree water variability. *J. Mar. Res.*, **40**(Suppl.), 757–775.

Tsuchiya, M., 1982: On the Pacific upper-water circulation. *J. Mar. Res.*, **40**(Suppl.), 777–799.

Young, W. R., and P. B. Rhines, 1982: A theory of wind-driven circulation II. Gyres with western boundary layers. *J. Mar. Res.*, **40**, 849–872.

Worthington, L. V., 1959: The 18° water in the Sargasso Sea. *Deep-Sea Res.*, **5**, 297–305.